Journal of Power Sources 196 (2011) 8881–8896

Contents lists available at ScienceDirect

Journal of Power Sources

journal homepage: www.elsevier.com/locate/jpowsour

Optimal operation management of fuel cell/wind/photovoltaic power sources connected to distribution networks

Taher Niknam [a], Abdollah Kavousifard [a], Sajad Tabatabaei [b,*], Jamshid Aghaei [a]

[a] Department of Electrical and Electronics Engineering, Shiraz University of Technology, Shiraz, P.O. 71555-313, Iran
[b] Department of Electrical Engineering, Mahshahr Branch, Islamic Azad University, Mahshahr, Iran

ARTICLE INFO

Article history:
Received 13 December 2010
Received in revised form 20 April 2011
Accepted 26 May 2011
Available online 6 June 2011

Keywords:
Modified honey bee mating optimization (MHBMO)
Distribution feeder reconfiguration (DFR)
Multiobjective optimization
Fuel cell
Wind energy
Photovoltaic (PV)
Renewable energy sources (RESs)

ABSTRACT

In this paper a new multiobjective modified honey bee mating optimization (MHBMO) algorithm is presented to investigate the distribution feeder reconfiguration (DFR) problem considering renewable energy sources (RESs) (photovoltaics, fuel cell and wind energy) connected to the distribution network. The objective functions of the problem to be minimized are the electrical active power losses, the voltage deviations, the total electrical energy costs and the total emissions of RESs and substations. During the optimization process, the proposed algorithm finds a set of non-dominated (Pareto) optimal solutions which are stored in an external memory called repository. Since the objective functions investigated are not the same, a fuzzy clustering algorithm is utilized to handle the size of the repository in the specified limits. Moreover, a fuzzy-based decision maker is adopted to select the 'best' compromised solution among the non-dominated optimal solutions of multiobjective optimization problem. In order to see the feasibility and effectiveness of the proposed algorithm, two standard distribution test systems are used as case studies.

1. Introduction

The application of the RESs such as wind, fuel cell and photovoltaic in the new competitive electric power markets has gained significant attention due to the economic and environmental concerns of fossils and nuclear fuel-based electricity energy as well as reduction of fossil resources [1]. Also, the existence of some important aspects as the quality of the RESs such as compatibility with other modular subsystem packages, fully automation possibility, low emission release, high efficiency and proper power quality and reliability have made them even more popular than before [2].

In recent years, so many researchers have attended to investigate the use of some kinds of renewable energies like wind energy, biogas energy, fuel cells, photovoltaic cells, combined heat and power systems (CHP), etc., in the distribution voltage level [3–6]. Nevertheless, there are some significant considerations to get use of the RESs appropriately and efficiently. Regions like offshore and high altitude areas that have more constant and stronger winds are suitable to be used for the construction of wind farms. The power stored in the airflows can be employed to rotate wind turbines and so generate a clean and consistent electric power. Fuel cell with a modular structure allows for simple construction and operation with possible applications for distributed and portable power generation [7]. Also as a result of their fast response, fuel cells have a good quality to follow and supply the load changes while maintaining the high efficiency at the same time [3–6]. Another new technology in the field of renewable energy technologies is photovoltaics (PV). PV is a method of generating electrical power by converting solar radiation into direct current electricity using semiconductors that exhibit the photovoltaic effect [8]. Like the other kinds of renewable energies, PV has found many applications including satellites, electric vehicles, remote dwelling, boats, on roofs, and by the use of DC–AC converters in the grids which are connected to the power system. All these applications and many other benefits that are not mentioned here make it critical to investigate the effect of the RESs on the distribution network especially in the area of the DFR problem.

Electric distribution networks are generally designed and constructed as the radial networks so as to have suitable and proper protection coordination. Nevertheless, the necessity of having a secure network, supplying all consumers, minimizing power losses and improving power quality, it is required to change the structure and the topology of the network using automatic or manual

Abbreviations: MHBMO, modified honey bee mating optimization; DFR, distribution feeder reconfiguration; PV, photovoltaic; FC, fuel cell; MOP, multiobjective optimization problem; MDFR, multiobjective DFR; RESs, renewable energy sources.

* Corresponding author at: Department of Electrical Engineering, Mahshahr Branch, Islamic Azad University, Mahshahr, Iran. Tel.: +98 711 7264121; fax: +98 711 7353502.
E-mail addresses: niknam@sutech.ac.ir, taher_nik@yahoo.com (T. Niknam), sdtabatabaei@gmail.com (S. Tabatabaei).

0378-7753/$ – see front matter © 2011 Elsevier B.V. All rights reserved.
doi:10.1016/j.jpowsour.2011.05.081

Nomenclature

X	state variables vector
n	number of state variables
N_{FC}	number of FC power sources
N_{PV}	number of PV power sources
N_{Wind}	number of wind power sources
N_b	number of branches
R_i	resistance of ith branch (Ω)
I_i	current of ith branch (A)
$P_{FC,i}$	active power production of the ith fuel cell power source (kW)
$P_{PV,i}$	active power production of the ith PV power source (kW)
$P_{Wind,i}$	active power production of the ith wind power source (KW)
P_{sub}	active power production of the substation (kW)
η_i	electrical efficiency of the ith FC
PLR_i	part load ratio of the ith FC
$C_{FC,i}$	cost of electrical energy generated by of the ith FC power source ($)
$C_{PV,i}$	cost of electrical energy generated by of the ith PV power source ($)
$C_{Wind,i}$	cost of electrical energy generated by of the ith Wind power source ($)
C_{sub}	cost of power generated at substation bus ($)
Price	cost of power per unit generated at substation bus ($)
Gr	annual rates of benefit
LF	loading factor
$E_{FC,i}$	emission of the ith FC power source (lb)
$E_{PV,i}$	emission of the ith PV power source (lb)
$E_{Wind,i}$	emission of the ith wind power source (lb)
E_{Grid}	emission of large scale sources (substation bus that connects to grid) (lb)
$NO_{xFC,i}$	nitrogen oxide pollutants of the ith FC power source (lb kWh^{-1})
$SO_{2FC,i}$	sulphur oxide pollutants of the ith FC power source (lb kWh^{-1})
$NO_{xPV,i}$	nitrogen oxide pollutants of the ith PV power source (lb kWh^{-1})
$SO_{2PV,i}$	sulphur oxide pollutants of the ith PV power source (lb kWh^{-1})
$NO_{xWind,i}$	nitrogen oxide pollutants of the ith wind power source (lb kWh^{-1})
$SO_{2Wind,i}$	sulphur oxide pollutants of the ith wind power source (lb kWh^{-1})
NO_{xGrid}	nitrogen oxide pollutants of the grid (kg)
SO_{2Grid}	sulphur oxide pollutants of the grid (kg)
$P_{min,FC,i}$	minimum active power of the ith FC power source (kW)
$P_{max,FC,i}$	maximum active power of the ith FC power source (kW)
$P_{min,PV,i}$	minimum active power of the ith PV power source (kW)
$P_{max,PV,i}$	maximum active power of the ith PV power source (kW)
$P_{min,Wind,i}$	minimum active power of the ith wind power source (kW)
$P_{max,Wind,i}$	maximum active power of the ith wind power source (kW)
$\lvert P_{ij}^{Line}\rvert$	absolute power flowing over distribution lines (kW)
$P_{ij,max}^{Line}$	maximum transmission power between the nodes i and j (kW)
$P_{ij,min}^{Line}$	minimum transmission power between the nodes i and j (kW)
V_{max}	maximum value of voltage magnitudes of ith bus (V)
V_{min}	minimum value of voltage magnitudes of ith bus (V)
$f_i(X)$	ith objective function
$J_i(X)$	equality constraints of ith objective function
$g_i(X)$	inequality constraints of ith objective function
f_i^{min}	lowest limit of ith objective function
f_i^{max}	highest limit of ith objective function
N_f	is the number of the objective functions in the MOP
$\mu_{fi}(X)$	membership function for ith objective function
D	drone
X_{queen}	best particle among the entire population or the queen
$X_{brood,j}$	the jth brood
Sp	queen spermatheca matrix
N_{Sp}	size of the queen spermatheca
$\Delta(f)$	absolute difference between the fitness of the drone and the fitness of the queen
α	speed reduction factor
γ	random value in the range of [0,1]
Prob(D)	probability of adding the sperm of drone D to the queen spermatheca
$S(t)$	queen speed
$F_i(X)$	values of the augmented $f_i(X)$
N_{eq}	number of equality constraints of the DFR problem
N_{ueq}	number of inequality constraints of the DFR problem
L_1	penalty factor
L_2	penalty factor
N_{ipop}	number of the bees
S_{queen}	queen speed
S_{max}	maximum speed of the queen
S_{min}	minimum speed of the queen
K_1	value of the production of NOx (lbk Wh^{-1})
K_2	values of the production of SOx (lbK Wh^{-1})
f_i^{queen}	the value of the ith objective function for the queen
f_i^{drone}	the value of the ith objective function for the drone
w_i	the weighting of the ith objective function
M_i	the mean value of the drones' population column-wise
m_i	the mean value of the ith element of the control vector in the drones' population column-wise
r_k	random value in the range of [0,1]
T_F	a constant factor which decides the value of mean to be changed. Can be 1or 2
$X_{q,k}$	the kth new queen generated for implementing modifying the breeding process
$X_{D,m}$	the mth new drone generated for implementing modifying the breeding process
round	the mathematic function which rounds each value to the nearest integer
rand( )	the function for the generation of random value
$Y_{k,m}$	the new individual generated through modification process
Z	the new individual generated through modification process

switches. However, the radial structure of the networks and discrete nature of the switches is a main obstacle to get use of the classical optimization methods in the multiobjective distribution feeder reconfiguration (MDFR) problem. Classical optimization methods have suggested transforming the multiobjective opti-

mization problem to a single objective optimization problem [9,10]. However, in these methods extensive computational resources (memories) are needed to find the multiple optima.

In the area of MDFR problem, Das [11] has presented a new multiobjective approach based on the fuzzy set theory to solve the DFR problem. Vanderson Gomes et al. have suggested a new heuristic method to change the configuration of the distribution systems [12]. Kim et al. [13] have suggested a new method based on neural network in order to identify the configuration of the network corresponding to different load levels. Taylor and Lubkeman [7] have presented an expert system to reduce the search space by the use of heuristic rules. Kashem et al. [14] have introduced a new algorithm based on the distance measurement to find a loop in the network, and then a switching plan is used to enhance the load balancing in the mentioned loop. Baran and Wu [15] have used a mixed integer programming (MIP) to solve the load balancing problem and power loss reduction in the network. In order to supply the purpose of load balancing and service restoration in two feeder networks, an algorithm based on the network reconfiguration has been presented by Zhou et al. [16]. Also, in [17,18] Niknam has proposed a method based on the evolutionary algorithms to convert multiobjective DFR problem to an equivalent augmented single objective problem. Here again too extensive computational resources and many runs are needed to find the solutions; therefore the efficiency of the algorithm will be reduced. Also, the new hybrid algorithm used by Niknam in [19] to solve the multiobjective DFR problem results in a single solution which does not observe the Pareto optimality concept. In fact it has the main disadvantage of ignoring many other good candidate solutions that can be supposed as optima.

In this paper a new modified honey bee mating evolutionary algorithm is utilized to solve MDFR problem while the effect of RESs is considered. The traditional HBMO suffered from two main shortcomings: (I) dependency on the algorithm parameters, and (II) the possibility of being trapped in local optima. Therefore, in this paper a new modification process is proposed to enhance the performance of the algorithm. Also, during the optimization process, the set of obtained non-dominated solutions, called Pareto-optimal solutions, are stored in the repository. In order to control the size of the repository, a fuzzy clustering technique is utilized.

2. Multiobjective DFR considering RESs

2.1. Objective functions

- *Minimization of the power losses*: Total power losses can be minimized by the following equation:

$$\begin{aligned} &f_1(X) = P_{\text{loss}}(X) = \sum_{i=1}^{N_{\text{br}}} R_i \times |I_i|^2, X = [\text{Tie}, \text{Sw}, P_g] \\ &\text{Tie} = [\text{Tie}_1, \text{Tie}_2, \text{Tie}_3, \ldots, \text{Tie}_{N_{\text{tie}}}]; \text{Sw} = [\text{Sw}_1, \text{Sw}_2, \text{Sw}_3, \ldots, \text{Sw}_{N\text{sw}}] \\ &P_{\text{FC}} = [P_{\text{FC},1}, P_{\text{FC},2}, \ldots, P_{\text{FC},N_{\text{FC}}}]; P_{\text{PV}} = [P_{\text{PV},1}, P_{\text{PV},2}, \ldots, P_{\text{PV},N_{\text{PV}}}] \\ &P_g = [P_{\text{FC}}, P_{\text{PV}}, P_{\text{Wind}}] \\ &P_{\text{Wind}} = [P_{\text{Wind},1}, P_{\text{Wind},2}, \ldots, P_{\text{Wind},N_{\text{Wind}}}] \end{aligned} \tag{1}$$

  where Tie_i and Sw_i are the states of the ith tie switch and sectionalizing switch which 0 and 1 are the values corresponding to open and close states, respectively.
- *Minimization of the voltage deviation of the buses*: This objective function can be defined as follows:

$$f_2(X) = \text{dev}(X) = \max[\left|1 - V_{\min}\right| \quad \text{and} \quad \left|1 - V_{\max}\right|] \tag{2}$$

  Minimization of the total cost of generation: The total cost is the summation of the cost related to the power produced by the grid and the cost related to the power produced by the RESs. The grid cost can be evaluated as follows:

$$C_{\text{sub}} = \text{price} \times P_{\text{sub}} \tag{3}$$

Table 1
Specifications of RESs (Test system 1).

	Capacity (kW)	Type	Location
RES 1	464.375	FC	6
RES 2	464.375	FC	13
RES 3	464.375	PV	19
RES 4	464.375	Wind energy	22

The cost of FC power sources can be evaluated as follows [20]:

$$\begin{aligned} &C_{\text{FC},i} = 0.04\,\$\text{kWh}^{-1} \times \frac{P_{\text{FC},i}}{\eta_i} \\ &\text{PLR}_i = \frac{P_{g,i}}{P_{\max_i}} \\ &\text{if} \quad \text{PLR}_i < 0.05 \Rightarrow \eta_i = 0.2716 \\ &\text{if} \quad \text{PLR}_i \geq 0.05 \Rightarrow \eta_i = 0.9033\,\text{PLR}_i^5 - 2.9996\,\text{PLR}_i^4 + 3.6503\,\text{PLR}_i^3 \\ &-2.0704\,\text{PLR}_i^2 + 0.3747 \end{aligned} \tag{4}$$

The cost of PV and wind units can be evaluated similarly by Eq. (5). The cost of generation of each kWh is a function of three parameters [21]: (I) investment cost; (II) operation and maintenance cost; (III) fuel cost.

$$\begin{aligned} &C_{\text{PV},i} = a + b \times P_{\text{PV},i} \\ &C_{\text{Wind},i} = a + b \times P_{\text{Wind},i} \\ &a = \frac{\text{Capital cost}(\$\text{kW}^{-1}) * \text{Capacity(kW)} * Gr}{\text{Life time(Year)} * 365 * 24 * \text{LF}} \\ &b = \text{Fuel cost}(\$\text{kWh}^{-1}) + O\&\text{MCost}(\$\text{kWh}^{-1}) \end{aligned} \tag{5}$$

Therefore the total cost is as follows:

$$f_3(X) = \text{Cost} = \sum_{i=1}^{N_{\text{FC}}} C_{\text{FC},i} + \sum_{i=1}^{N_{\text{PV}}} C_{\text{PV},i} + \sum_{i=1}^{N_{\text{Wind}}} C_{\text{Wind},i} + C_{\text{sub}} \tag{6}$$

Minimizing the total emission produced: The total emission of the grid and the RESs is as follows:

$$\begin{aligned} &f_4(X) = \text{Emission} = \sum_{i=1}^{N_{\text{FC}}} E_{\text{FC},i} + \sum_{i=1}^{N_{\text{PV}}} E_{\text{PV},i} + \sum_{i=1}^{N_{\text{Wind}}} E_{\text{Wind},i} + E_{\text{Grid}} \\ &E_{\text{FC},i} = \text{NO}x_{\text{FC},i} + \text{SO2}_{\text{FC},i} = (K_1^{\text{FC},i} + K_2^{\text{FC},i})^{\text{lb MWh}^{-1}} \times P_{\text{FC},i} \\ &E_{\text{PV},i} = \text{NO}x_{\text{PV},i} + \text{SO2}_{\text{PV},i} = (K_1^{\text{PV},i} + K_2^{\text{PV},i})^{\text{lb MWh}^{-1}} \times P_{\text{PV},i} \\ &E_{\text{Wind},i} = \text{NO}x_{\text{Wind},i} + \text{SO2}_{\text{Wind},i} = (K_1^{\text{Wind},i} + K_2^{\text{Wind},i})^{\text{lb MWh}^{-1}} \\ &\quad \times P_{\text{Wind},i} \\ &E_{\text{Grid}} = \text{NO}x_{\text{Grid}} + \text{SO2}_{\text{Grid}} = (K_1^{\text{Grid}} + K_2^{\text{Grid}})^{\text{lb MWh}^{-1}} \times P_{\text{sub}} \end{aligned} \tag{7}$$

The relevant values of these parameters are brought in Table 2.

2.2. Limits and constraints

(i) Limits associated with distribution lines:

$$P_{ij,\min}^{\text{Line}} < P_{ij}^{\text{Line}} < P_{ij,\max}^{\text{Line}} \tag{8}$$

(ii) Distribution power flow equations:

$$\begin{aligned} P_i &= \sum_{i=1}^{N_{\text{bus}}} V_i V_j Y_{ij} \cos(\theta_{ij} - \delta_i + \delta_j) \\ Q_i &= \sum_{i=1}^{N_{\text{bus}}} V_i V_j Y_{ij} \sin(\theta_{ij} - \delta_i + \delta_j) \end{aligned} \tag{9}$$

This equation is a load flow equation that plays the role of an equality constraint.

(iii) Keeping the radial structure: since the distribution networks are supposed to be radial, this quality of the network should be

Table 2
Emission factors related to NO_x, CO_2 and SO_2.

Emission factors (lb MWh^{-1})							
Emission type	Grid	Gas turbine	Micro turbine	Wind	PV	FC	Internal combustion (IC)
NO_x	5.06	0.03	0.44	0	0	1.15	4.7
CO_2	2031	1078	1596	0	0	1108	1432
SO_2	7.9	0.006	0.008	0	0	0.008	0.454

preserved during the reconfiguration. Each loop in the network is composed of a tie switch and a sectionalizing switch that each time that one is open; the other one is closed, so that a radial network would be achieved.

(iv) Feeder current limitation [22]:

$$|I_{f,i}| \le I_{f,i}^{\max}; \quad i = 1, 2, \ldots, N_f \tag{10}$$

(v) RESs constraints on active power production:

$$p_{\min,FC,i} \le p_{FC,i} \le p_{\max,FC,i}; p_{\min,PV,i} \le p_{PV,i} \le p_{\max,PV,i};$$
$$p_{\min,Wind,i} \le p_{Wind,i} \le p_{\max,Wind,i} \tag{11}$$

(vi) Bus voltage constraints:

$$V_{\min} \le V_i^t \le V_{\max} \tag{12}$$

3. Modeling of the RESs

3.1. Fuel cell

FC has been among of the most important developments in the field of power generation in recent years. Because of their cleanness, good efficiency and high reliability, they have become one of the most attractive power supply sources in the field of distributed generation and electrical vehicles [23,24]. There are many different kinds of FCs according to their different characteristics. The solid oxide fuel cells (SOFCs) and molten carbonate fuel cells (MCFCs) are supposed to be in the high-temperature category of the FCs. Their higher efficiency and lower operation cost is considerable in comparison to the conventional power plants in the megawatt range of production [24]. The typical efficiency of conventional power plants ranges from 38% to 40%, whereas the efficiency of an SOFC is in the range of 55–60% [25]. Another kind of FC is the proton exchange membrane FC (PEMFC) which has the ability of operation at the air temperature allowing rapid startup [23]. The PEMFC efficiency is around 40–60% with the power and voltage ability to meet special demands as a result of its modularity structure.

3.2. Photovoltaic

Solar photovoltaics (PVs) are arrays of cells containing a material that converts solar radiation into direct current (DC) electricity [8]. Solar photovoltaic (SPV) electric power generation is a promising clean technology with vast potential [26]. Orbiting satellites were the first practical application of PVs. But today so much attention is paid to use them as a source of power in the power generation grids. As the PV cell temperature exceeds a threshold of 45 °C, the PV performance decreases [8]. In this situation the PVs performance as renewable energy power source should be investigated in different condition carefully.

3.3. Wind

The performance of the wind turbines is based on the conversion of the kinetic energy of wind into electricity. The instantaneous power produced by a turbine is proportional to the third power of the instantaneous wind speed [8]. Therefore as the wind speed increases, the output power increases dramatically. As mentioned before, regions like offshore, open flat areas and high altitude areas that have more constant and stronger winds are suitable to be used for the construction of wind farms.

3.4. Modeling of the renewable energy power plants

RESs can be modeled by two types: (I) constant voltage magnitude, constant active power loads; (II) constant active and reactive power loads. When the renewable energy power source is supposed to be constant active power and voltage magnitude load model, it should be able to keep its voltage magnitude constant by the injection of reactive power. When the renewable energy power source is considered as a constant active and reactive power load model, a specific active and reactive power is produced and injected to the network. However, in both cases it should be considered that active and reactive power produced should not exceed the generation capacity. As the result of the structure of the distribution networks, the load distribution in these networks is unbalanced. So the RESs operation and control is done in two forms: (I) simultaneous three phase; (II) independent three-phase control or single phase control. Therefore according to their model and type of control, four models can be defined for these generators (Fig. 1) [7]:

(I) Constant active and reactive load model with simultaneous three-phase control.
(II) Constant reactive power and voltage magnitude load model with simultaneous three-phase control.

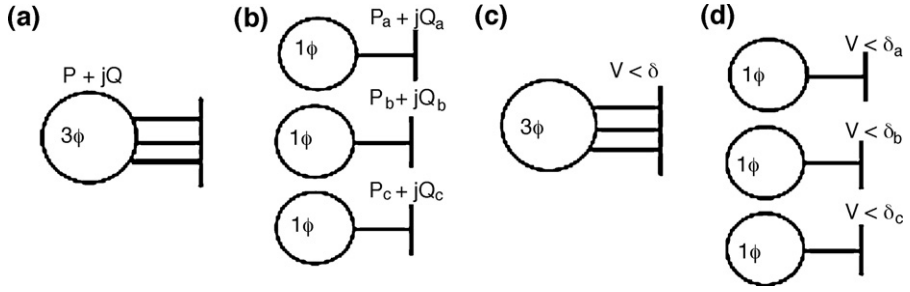

Fig. 1. Models of RESs: (a) constant active and reactive load model with simultaneous three-phase control, (b) constant active and reactive load model with independent three-phase control, (c) constant active power and voltage magnitude load model with simultaneous three-phase control and (d) constant active power and voltage magnitude load model with independent three-phase control.

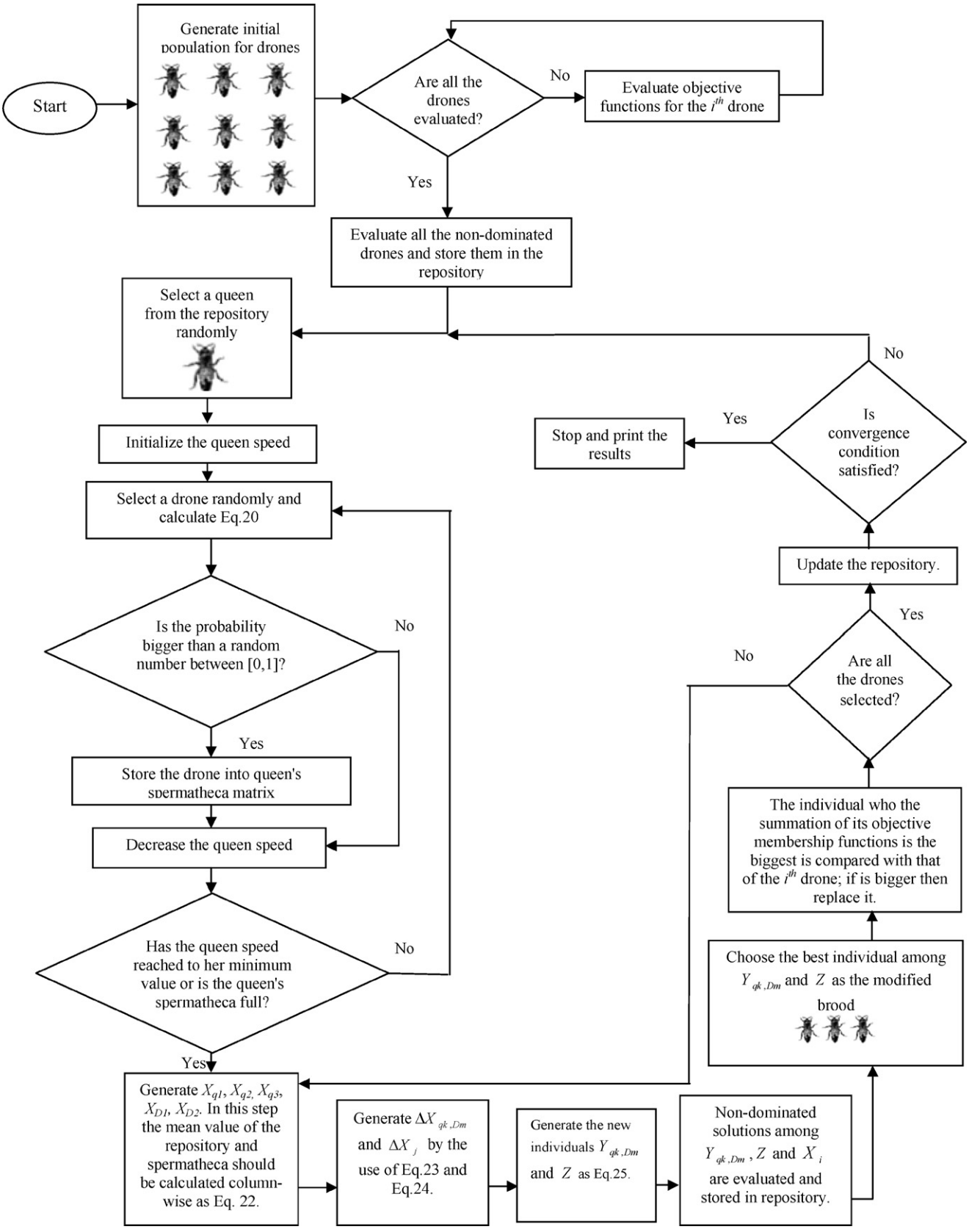

Fig. 2. Block diagram of MHBMO algorithm.

Table 3
Comparison of active power losses objective functions evaluated by different methods neglecting RESs (Test system 1).

Method	Power loss [kW]	Minimum voltage	Open switches
Goswami and Basu [29]	139.53	0.93781964	s7,s9,s14,s32,s37
Vanderson Gomes et al. [30]	139.53	0.93781964	s7,s9,s14,s32,s37
PSO-SFLA [31]	139.53	0.93781964	s7,s9,s14,s32,s37
MSFLA [32]	139.53	0.93781964	s7,s9,s14,s32,s37
Shirmohammadi and Hong [33]	140.26	0.93781964	s7,s10,s14,s32,s37
The proposed algorithm	139.53	0.93781964	s7,s9,s14,s32,s37

Table 4
Comparison of voltage deviation objective functions evaluated by different methods neglecting RESs (Test system 1).

Method	Voltage deviation [p.u]	Minimum voltage	Open switches
GA	0.06218097	0.93781902	s7,s10,s14,s32,s37
PSO	0.06120031	0.93879681	s6,s9,s14,s32,s37
HBMO	0.06266643	0.93733335	s9,s12,s19,s35,s37
The proposed algorithm	0.06120031	0.93879681	s7,s9,s14,s32,s37

(III) Constant active and reactive load model with independent three-phase control.
(IV) Constant reactive power and voltage magnitude load model with independent three-phase control.

4. Methodology

Multiobjective optimization problem (MOP) is the process of optimizing some different conflicting objective functions simultaneously when all the constraints and the limitations are observed and the best optimized solution for all the objective functions are achieved. MOP can be defined as [22]:

$$\begin{aligned} &\min\ F = [f_1(X), f_2(X), \ldots, f_n(X)]^T \\ &s.t. \\ &g_i(X) < 0 \quad i = 1, 2, \ldots, N_{\text{ueq}} \\ &h_i(X) = 0 \quad i = 1, 2, \ldots, N_{\text{eq}} \end{aligned} \tag{13}$$

In this essay X is the variable vector of making decision. Also n is the number of objective functions.

$$X = [\text{Tie}, \text{Sw}, P_g] \tag{14}$$

In fact the main difference between the single and the multiobjective optimization problem is the ability of the MOP in observing the best optimal solution of different objective functions simultaneously. This feature is due to capability of MOP in selection of the solutions as a set of Pareto points. In MOP problem X^* is called a Pareto optimal solution if it is impossible to find a solution X in Ω such that X dominates $X^* \in \Omega$. Ω is the set of all the vectors (X) that observe the constraints and limitations.

In definition the solution X_1 dominates X_2 if the following two conditions are satisfied:

$$\begin{aligned} &(1)\forall\, j \in \{1, 2, \ldots, n\}, f_j(X_1) \le f_j(X_2) \\ &(2)\exists\, k \in \{1, 2, \ldots, n\}, f_k(X_1) < f_k(X_2) \end{aligned} \tag{15}$$

5. Fuzzy-based clustering

When the optimization is started, in each iteration, the best values of the objective functions are evaluated. However, the big difference which exists between the optimal value of some of the objective functions and the optimal value of the other ones is a barrier for making the improvement rate similar to each other. The main point of using fuzzy set theory in this investigation is to bring all the optimal values of the objective functions in the same base, so that to create a good criterion for comparison. The membership function designated to each objective function is as follows:

$$\mu_{f_i}(X) = \begin{cases} 1 & \text{for } f_i(X) \le f_i^{\min} \\ 0 & \text{for } f_i(X) \ge f_i^{\max} \\ \dfrac{f_i^{\max} - f_i(X)}{f_i^{\max} - f_i^{\min}} & f_i^{\min} \le f_i(X) \le f_i^{\max} \end{cases} \tag{16}$$

As we see the membership functions used here are continuous functions with lower and upper limits which decrease monotonically.

Table 5
Comparison of objective functions evaluated by different methods considering RESs for 25 trails on Test system 1.

Objective function	Method	Average	Standard deviation	Worst solution	Best solution	Open switches of best solution	CPU time [s]
Power losses [kW]	GA	95.435466	3.774	104.12418	92.273284	s7,s10,s31,s34,s37	13.924
	PSO	89.975333	1.916	95.265620	89.089835	s6,s8,s32,s34,s37	12.785
	HBMO	92.548024	2.115	98.333334	91.103298	s6,s8,s34,s36,s37	13.234
	The proposed algorithm	85.583101	00.00	85.583101	85.583101	s7,s11,s31,s34,s37	10.031
Voltage deviation [p.u]	GA	0.05487009	0.002391	0.06104787	0.05291578	s7,s9,s13,s32,s37	11.593
	PSO	0.05083480	0.001547	0.05444417	0.04920617	s11,s13,s35,s36,s37	10.319
	HBMO	0.05120344	0.0021054	0.05851443	0.05114542	s6,s13,s21,s32,s37	11.043
	The proposed algorithm	0.04898826	0.0000000	0.04898826	0.04898826	s11,s31,s33,s34,s37	9.303
Cost [$]	GA	155.16237	0.426	155.85994	154.98564	s6,s9,s34,s36,s37	12.776
	PSO	154.43350	0.235	155.07246	154.33555	s7,s11,s14,s36,s37	11.350
	HBMO	154.68270	0.275	155.35477	154.39087	s7,s11,s34,s36,s37	11.945
	The proposed algorithm	154.18182	0.000	154.18182	154.18182	s7,s9,s14,s32,s37	10.500
Emission [lb]	GA	27,587.566	362.34	28,046.59	27,298.962	s21,s28,s33,s32,s37	12.245
	PSO	27,376.903	347.63	26,878.888	25,747.949	s12,s20,s35,s36,s37	10.694
	HBMO	27,440.376	351.38	27,523.738	26,357.004	s9,s33,s34,s36,s37	11.404
	The proposed algorithm	25,280.766	000.00	25,280.766	25,280.766	s7,s8,s32,s35,s37	9.484

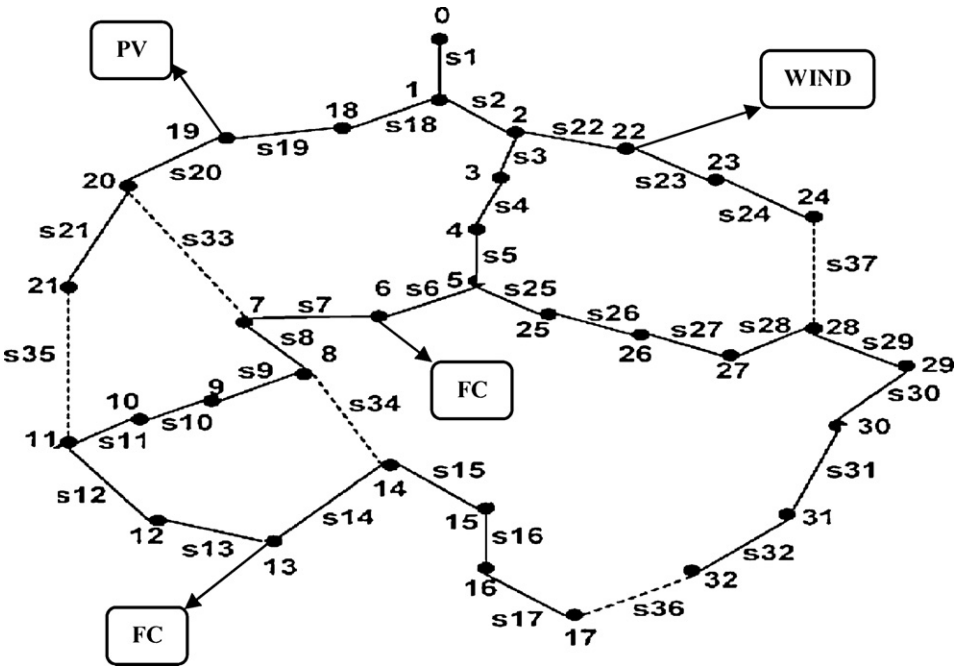

Fig. 3. Single line diagram of 32 bus test system.

For each of the solutions in the repository, the normalized membership function can be evaluated as follows:

$$N_\mu(j) = \frac{\sum_{i=1}^{n} \omega_i \times \mu_{fl}(X_j)}{\sum_{j=1}^{m}\sum_{i=1}^{n} \omega_i \times \mu_{fl}(X_j)} \quad (17)$$

where n is the number of the objective functions and m is the number of the individuals in the repository. This equation makes a type of decision making criteria which is adaptive and has the ability of applying the decision maker's options. For the controlling the size of the repository, all the weighting factors (w_i) are set unit. Therefore N_μ for all the non-dominated solutions is evaluated and the best solutions are kept in the repository. In this paper we get advantage of fuzzy clustering in another application too. In the simulation results, it is explained that by changing the weighting factors to a different value than 1, the preferences of the operator in determining the importance of the objective functions can be achieved.

6. Honey bee mating optimization (HBMO) modeling

6.1. Original HBMO

In the natural world, these types of flying insects (honey bees) live with each other as a colony. That is their life has a direct relation with their social colony. The communication of these insects structurally is composed of three main groups: the queen (female), the drones (male) and the workers. The process of mating between a drone and a queen is done probabilistically by using an annealing function as follows [27]:

$$\text{prob}(D) = \exp\left(-\frac{\Delta f}{S(t)}\right) \quad (18)$$

If the mating process is done successfully, the drone sperm is stored in the queen spermatheca. After each mating, the queen speed decreases as follows:

$$S(t+1) = \alpha \times S(t) \quad (19)$$

This mating process continues until the time that the queen's spermatheca becomes full or her speed deceases to a specific value. After generating the new broods, they should be protected and improved by the workers (for a complete description see [27,28]). As a matter of fact, the new generation is consisted of all the new solutions that should be used in the optimization process. However, if one of these broods has a better situation than the queen's, then it replaces the queen and another new generation is created by the use of the new queen. This process is continued until the time that the best queen is achieved.

6.2. Modified HBMO (MHBMO) algorithm

As we mentioned earlier, original HBMO suffers from the probability of being trapped in local optima. This shortcoming roots from the mating process. As we said in the last section, the process of mating between a drone and a queen in the original HBMO is done probabilistically by using Eq. (18). However, in the MHBMO algorithm, each queen value is composed of the all value of the objective

Table 6
Some of the non-dominated-solution found for MDFR problem (Test system 1).

	Power losses (kW)	Voltage deviation (p.u)	Cost ($)	Emission (lb)
1	085.583	0.053385	158.060	26,215.79
2	092.296	0.054754	157.705	29,083.56
3	089.471	0.058755	157.026	31,569.95
4	119.517	0.060206	155.648	36,982.22
5	108.316	0.055584	156.445	34,074.18
6	094.805	0.048988	158.429	25,335.31
7	141.097	0.066092	154.437	48,966.26
8	106.231	0.055065	156.207	35,622.73
9	097.291	0.049462	157.391	31,977.56
10	094.752	0.056561	157.840	27,501.51
11	121.030	0.062998	159.305	26,457.16
12	113.175	0.056907	155.816	35,854.27
13	098.836	0.057267	156.827	33,453.47
14	139.533	0.062180	154.181	49,954.62
15	100.242	0.055331	158.113	27,610.90
16	103.064	0.053654	156.429	34,186.32
17	090.596	0.054528	158.260	25,280.76
18	108.522	0.060597	156.552	32,554.66
19	124.000	0.057638	155.324	38,607.39
20	112.660	0.056966	155.640	38,336.96

functions which are considered in the problem. Therefore the in the proposed method, Eq. (18) is developed as follows:

$$\text{prob}(D) = \exp\left(-\frac{\Delta f}{S(t)}\right)$$
$$\Delta f = \sqrt{(f_1^{\text{queen}} - f_1^{\text{drone}})^2 + (f_2^{\text{queen}} - f_2^{\text{drone}})^2 + (f_3^{\text{queen}} - f_3^{\text{drone}})^2 + \dots} \quad (20)$$

In the original HBMO each brood is produced by the following equation:

$$X_{\text{queen}} = [x_{q,1}, x_{q,2}, \dots, x_{q,N}]$$
$$Sp_i = [s_{i,1}, s_{i,2}, \dots s_{i,N}],\ i = 1, 2, \dots, N_{Sp} \quad (21)$$
$$X_{\text{brood},j} = X_{\text{queen}} + \gamma \times (X_{\text{queen}} - Sp_i)$$

As we can see, in the original HBMO, one queen will mate with the drones' population to generate the new broods. But in the proposed MHBMO algorithm, in order to enhance the diversity of the new generation of the honey bees (broods), after generation of the queen spermatheca in a similar method to the original HBMO, the breeding process is corrected as the following. Note it that this process should be repeated for all the drones (X_i).

Firstly, three new individual should be generated as the new queens for implementing breeding process. The first individual (X_{q1}) is selected from the repository randomly. For the generation of the second individual, the mean value of the repository is calculated column-wise, which gives the mean value of each particular individual as:

$$M_i = [m_1, m_2, m_3, \dots, m_n] \quad (22)$$

Note it that M_i which is generated here is selected as the new second queen (X_{q2}). The third modified queen (X_{q3}) is generated by the use of fuzzy membership function. That is the individual in the repository which the summation of its membership function values is the most (so the best solution) is the selected as the third modified queen.

After selection of the new three queens, two individual should be generated as the new drones for implementing breeding process. The first new drone is the mean value of the queen spermatheca which is calculated column-wise. The second new drone is selected from the population of the drones randomly. The idea which is used here for the modification process is to move X_i toward the corresponding state vector of the queen. In fact since the queen position is the best, so by moving the position of each individual toward the queen's position, the position of the specified individual will be improved. Now, by the use $X_{q1}, X_{q2}, X_{q3}, X_{D1}$ and X_{D2}, six ΔX_i($\Delta X_{q,i}$, $\Delta X_{D,i}$) are produced as the follows:

$$\Delta X_{qk,Dm} = r_k(X_{q,k} - T_F X_{D,m}); \quad k = 1, 2, 3, \quad m = 1, 2 \quad (23)$$

Here T_F is a constant factor which decides the value of mean to be changed. T_F can takes two values of 1 and 2 which is determined heuristically as: T_F = round[1 + rand(0,1)]. For improving the diversity of the search space a drone X_j is selected from the population of the drones such that $X_j \neq X_i$. Then by the use of the following equation ΔX_j is determined as:

$$\begin{aligned}&\text{if } f(X_j) \geq f(X_i)\\ &\quad \Delta X_j = \text{rand}(.) \times (X_j - X_i)\\ &\text{else}\\ &\quad \Delta X_j = \text{rand}(.) \times (X_i - X_j)\\ &\text{end}\end{aligned} \quad (24)$$

where rand(.) is a random function generator. The new six modified individuals are generated as follows:

$$Y_{k,m} = X_i^{old} + \Delta X_{qk,Dm}; \quad k = 1, 2, 3, \quad m = 1, 2$$
$$Z = X_i^{old} + \Delta X_j \quad (25)$$

Now by the use of Eq. (15), the non-dominated solutions among $Y_{1,1}$, $Y_{1,2}$, $Y_{2,1}$, $Y_{2,2}$, $Y_{3,1}$, $Y_{3,1}$ and Z are evaluated and stored in the repository. If there is only one non-dominated solution among them, then this individual is selected as the modified brood. Nevertheless if there is more than one non-dominated solution among the individuals, then the individual which the summation of its membership function is the most (so the most satisfying) is selected as the new modified brood. For every individual in the population of drones, this process should be repeated. After that the breeding process for all the drones is completed then the repository is updated by Eq. (15).

Another significant difference between the MHBMO algorithm and the original HBMO algorithm is in the generation of the new drones' population. In the original HBMO, after choosing the new queen from the broods' population then the old drone generation is discarded. In the MHBMO algorithm, each individual of the new drones' population is generated during the breeding process. As mentioned before, for each drone, seven new modified broods are generated. After each breeding process, the non-dominated solution which the summation of its membership function values is the most (and therefore the best brood) is compared with that of the corresponding drone (X_i). If the summation of the best brood membership function is better than that of X_i, then replace it, else X_i will be kept in its position. So after a complete breeding process, the new drones' population is updated. The MHBMO algorithm is depicted in Fig. 2.

6.3. Solution procedure of MDFR considering RESs

Step 1: Defining the input data.

Step 2: Converting the constrained MOP to an unconstrained one: here the constrained MOP should be changed to an unconstrained one by constructing an augmented objective function as Eq. (26). Since all constrains must be met, so penalty factors L1 and L2 are used to prevent violating the constraints.

$$F(X) = \begin{bmatrix} F_1(X) \\ F_2(X) \\ F_3(X) \\ F_4(X) \end{bmatrix}_{4\times 1} = \begin{bmatrix} f_1(X) + L_1 \sum_{i=1}^{N_{eq}} (J_i(X))^2 + L_2 \left(\sum_{i=1}^{N_{ueq}} (\text{Max}[0, -g_i(X)])^2 \right) \\ f_2(X) + L_1 \sum_{i=1}^{N_{eq}} (J_i(X))^2 + L_2 \left(\sum_{i=1}^{N_{ueq}} (\text{Max}[0, -g_i(X)])^2 \right) \\ f_3(X) + L_1 \sum_{i=1}^{N_{eq}} (J_i(X))^2 + L_2 \left(\sum_{i=1}^{N_{ueq}} (\text{Max}[0, -g_i(X)])^2 \right) \\ f_4(X) + L_1 \sum_{i=1}^{N_{eq}} (J_i(X))^2 + L_2 \left(\sum_{i=1}^{N_{ueq}} (\text{Max}[0, -g_i(X)])^2 \right) \end{bmatrix}_{4\times 1} \quad (26)$$

L_1 and L_2 as the penalty factors are supposed to be 10^5 in the paper.

Step 3: Initial population generation. The initial population is as follows:

$$\text{initial\_population} = \begin{bmatrix} X_1 \\ X_2 \\ \dots \\ X_{N_{\text{ipop}}} \end{bmatrix}_{N_{\text{ipop}} \times (N_{\text{tie}} + N_{\text{sw}} + N_g)} \quad (27)$$

$$X_i = [x_i] = [\text{Tie}_i, \text{Sw}_i, P_{g,i}]$$

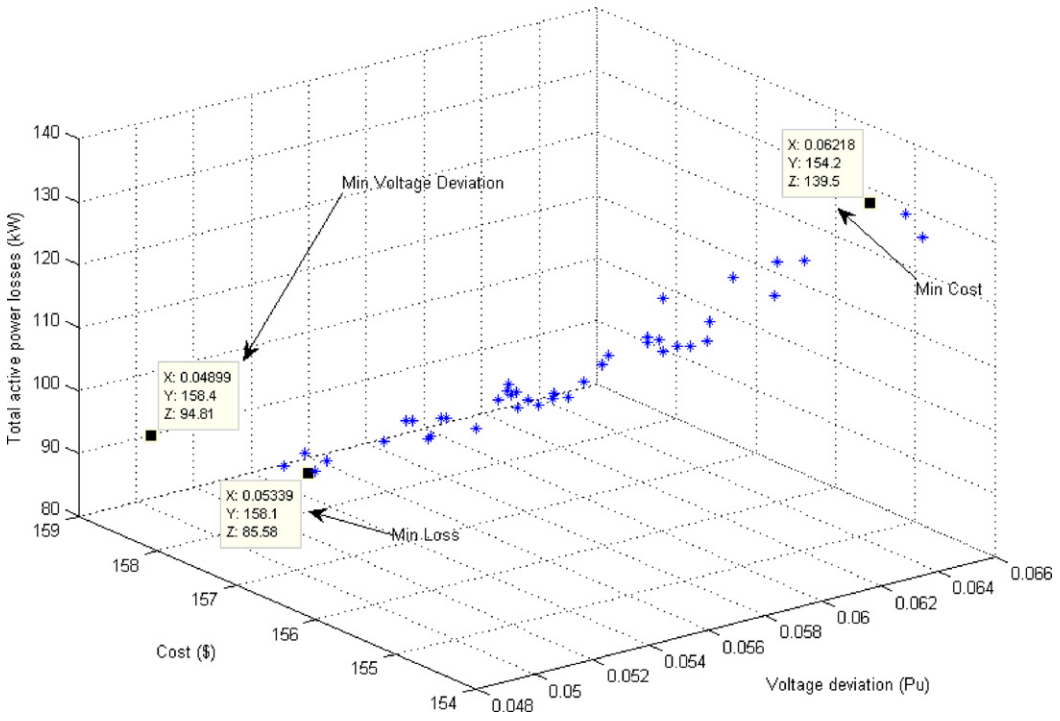

Fig. 4. 3D plot of the Pareto-optimal solutions found for case study 1 considering total active power losses, voltage deviation and cost objective functions.

$$\text{Tie} = [\text{Tie}_1, \text{Tie}_2, \text{Tie}_3, \ldots, \text{Tie}_{N_{\text{Tie}}}],$$

$$\text{Sw} = [\text{Sw}_1, \text{Sw}_2, \text{Sw}_3, \ldots, \text{Sw}_{N_{\text{Sw}}}]$$

$$P_g = [P_{\text{FC}}, P_{\text{PV}}, P_{\text{Wind}}], \quad P_{\text{FC}} = [P_{\text{FC},1}, P_{\text{FC},2}, \ldots, P_{\text{FC},N_{\text{FC}}}]$$

$$P_{\text{PV}} = [P_{\text{PV},1}, P_{\text{PV},2}, \ldots, P_{\text{PV},N_{\text{PV}}}], \quad P_{\text{Wind}} = [P_{\text{Wind},1}, P_{\text{Wind},2}, \ldots, P_{\text{Wind},N_{\text{FC}}}], \quad i = 1, 2, 3, \ldots, N; \quad N_g = N_{\text{PV}} + N_{\text{FC}} + N_{\text{Wind}}$$

Step 4: Objective function evaluation. After generating the initial population, load flow is carried on, and all the membership functions related to the objective functions are evaluated by Eq. (16).

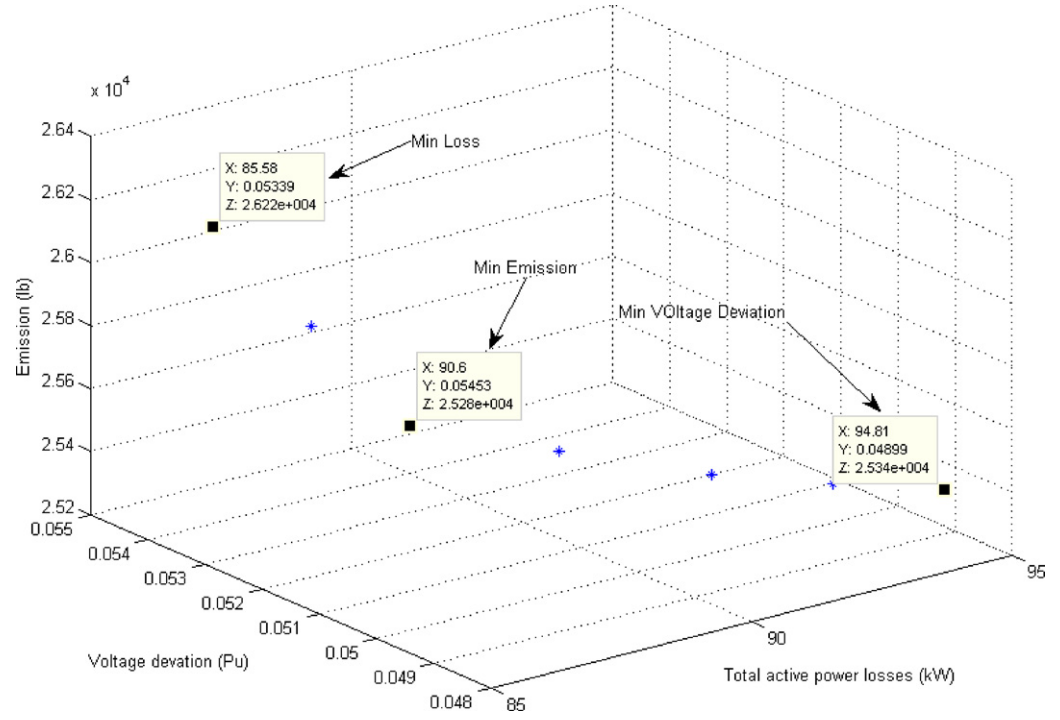

Fig. 5. 3D plot of the Pareto-optimal solutions found for case study 1 considering total active power losses, voltage deviation and emission objective functions.

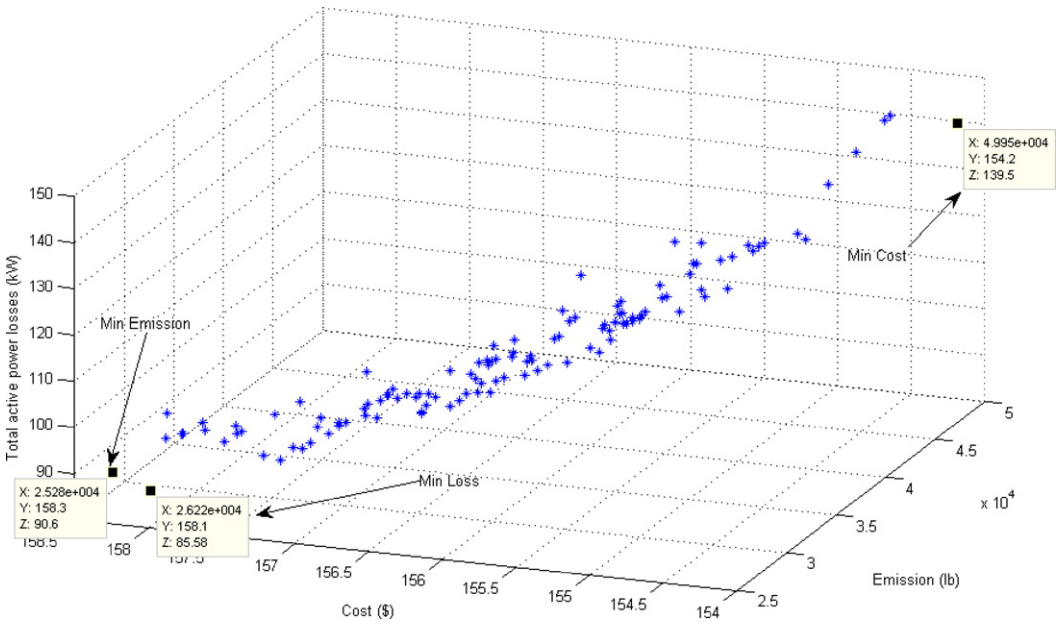

Fig. 6. 3D plot of the Pareto-optimal solutions found for case study 1 considering total active power losses, cost and emission objective functions.

Here $\mu_{p_{\text{loss}},i}(X)$, $\mu_{d_{\text{voltage}},i}(X)$, $\mu_{\text{price},i}(X)$ and $\mu_{\text{Emission},i}(X)$ are membership functions of the total power losses, the voltage deviation, the total cost and the total emission for the ith individual in the population.

Step 5: Repository complement. Here by the use of membership functions evaluated in the last step and by the use of Eq. (15), all the non-dominated solutions are found and stored in the repository.

Step 6: Queen selection. A queen is selected from the non-dominated solutions stored in the repository randomly.

Step 7: Generation of the queen spermatheca matrix. At the start of mating, the queen flies by her maximum speed. Then a drone is chosen from the population randomly. Then a random number between zero and one is generated. If this random number is less than the mating probability evaluated by Eq. (20), then the drone sperm is added to the queen spermatheca, else another drone is chosen randomly and the process is repeated.

Step 8: Breeding process and updating drones' population: the breeding process should be implemented as it was described in Section 6.2 by the use of Eqs. (22)–(25). After the termination of the breeding process, the repository

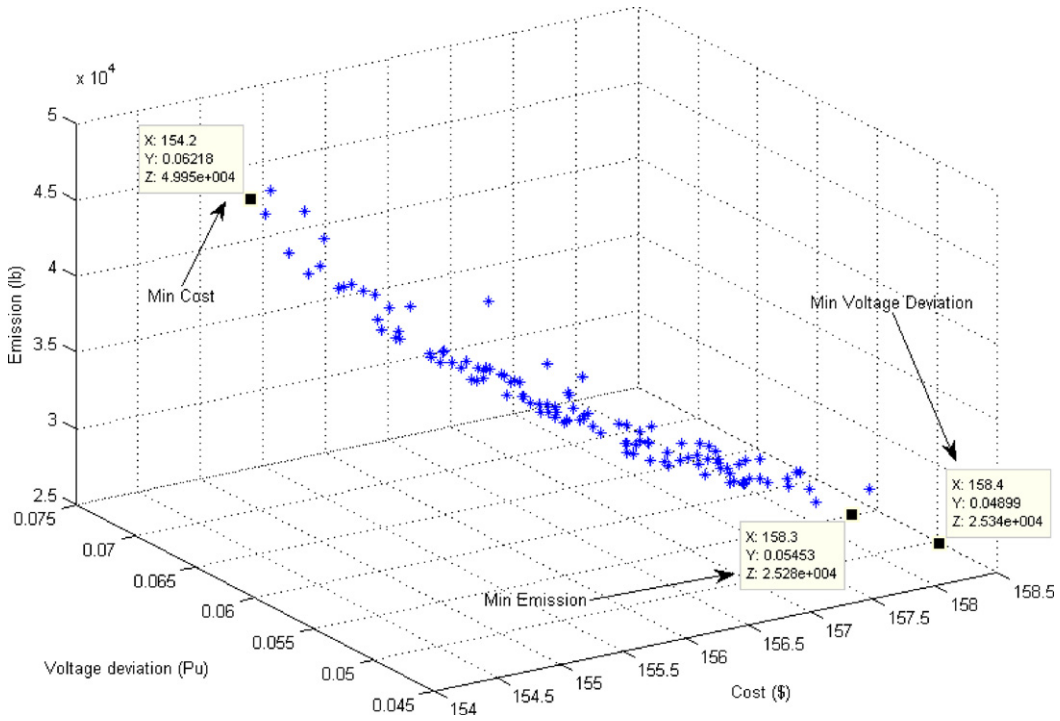

Fig. 7. 3D plot of the Pareto-optimal solutions found for case study 1 considering emission, voltage deviation and cost objective functions.

Table 7
Objective function values in all cases (Test system 1).

Cases	Importance				f_1	f_2	f_3	f_4
	w_1	w_2	w_3	w_4				
Case I	–	–	–	–	85.583	0.053385	158.060	26,215.79
Case II	–	–	–	–	94.805	0.048988	158.429	25,335.31
Case III	–	–	–	–	139.533	0.062180	154.181	49,954.62
Case IV	–	–	–	–	90.596	0.054528	158.260	25,280.76
Case V	0.33	0.33	0.33	0	101.460	0.052126	156.191	–
	0.25	0.25	0.5	0	110.788	0.054349	155.402	–
	0.25	0.5	0.25	0	92.863	0.051337	156.992	–
	0.5	0.25	0.25	0	92.863	0.051337	156.992	–
Case VI	0.33	0	0.33	0.33	85.583	–	158.060	26,215.79
	0.25	0	0.25	0.5	85.583	–	158.060	26,215.79
	0.25	0	0.5	0.25	104.620	–	156.356	32,808.73
	0.5	0	0.25	0.25	85.583	–	158.060	26,215.79
Case VII	0	0.33	0.33	0.33	–	0.050984	157.698	27,776.86
	0	0.25	0.25	0.5	–	0.050984	157.698	27,776.86
	0	0.25	0.5	0.25	–	0.055561	155.870	35,197.85
	0	0.5	0.25	0.25	–	0.050984	157.698	27,776.86
Case VIII	0.33	0.33	0	0.33	94.805	0.048988	–	25,335.31
	0.25	0.25	0	0.5	94.805	0.048988	–	25,335.31
	0.25	0.5	0	0.25	94.805	0.048988	–	25,335.31
	0.5	0.25	0	0.25	85.583	0.053385	–	26,215.79
Case IX	0.25	0.25	0.25	0.25	94.805	0.0489880	158.429	25,335.31
	0.2	0.2	0.2	0.4	94.805	0.0489880	158.429	25,335.31
	0.2	0.2	0.4	0.2	96.610	0.051103	156.957	30,392.10
	0.2	0.4	0.2	0.2	94.805	0.048988	158.429	25,335.31
	0.4	0.2	0.2	0.2	85.583	0.053385	158.060	26,215.79

should be updated. During each breeding for X_i (the ith drone), the position of X_i is updated as described in Section 6.2.

Step 9: If all the drones are checked go to the next step, else go to step 8.

Step 10: Updating the repository. In this step the repository is checked so that all the solutions stored in the repository will be non-dominated solutions.

Step 11: Updating the queen. A new queen is chosen from the updated repository randomly.

Step 12: Generating the queen speed. The queen speed is generated as:

$$(28) S_{\text{queen}} = \text{rand}(.) \times (S_{\max} - S_{\min}) + S_{\min}$$

Step 13: Termination criterion. If the number of iterations reaches to maximum number of the iteration, finish the algorithm, else go to step 6.

7. Simulation results

In this section the proposed method is examined on two distribution networks as case studies.

Table 8
Specifications of RESs (Test system 2).

	Capacity (kW)	Type	Location
RES 1	500	FC	6
RES 2	500	FC	53
RES 3	500	Wind energy	13
RES 4	500	Wind energy	60
RES 5	500	Wind energy	18
RES 6	500	PV	71
RES 7	500	PV	2

7.1. Case study 1

The first test system is a 12.66 kV system which consists of 32 buses, 5 sectionalizing switches and 5 tie switches [15]. The initial power loss before the reconfiguration is 202.67 kW. Table 1 shows the location, capacity, and type of RESs. Also, the emission factors related to NO_x, CO_2 and SO_2 are shown in Table 2. The single diagram of the network is illustrated in Fig. 3.

Since MHBMO algorithm is used in this paper for the first time to solve DFR problem, then first of all, a single objective optimization of the first two objective functions (total active power losses and voltage deviation) is evaluated to compare the performance of the MHBMO algorithm with the other methods in the area. The results of comparison between the performance of the proposed method and some famous evolutionary algorithms like particle swarm optimization (PSO) algorithm, genetic algorithm (GA), honey bee mating optimization (HBMO), etc., are shown in the following. The superiority of the proposed method over the other evolutionary algorithms can be deduced easily from Tables 3 and 4. In these tables, the single objective DFR is evaluated while the RESs are neglected. It is obvious that the total power losses and the voltage deviation objective functions which are evaluated by the proposed method are more satisfying than the results of the other algorithms and the good ability of the algorithm can be inferred. In Table 5, the effect of RESs on the DFR problem is investigated. It is evident that the amount of pollution generated by the total system will be decreased in the presence of the RESs. On the other hand, the use of these sources of energy in the system has resulted to a considerable improvement of the other three objective functions' values. In order to have a more precise comparison, the average value, standard deviation and the worst solution evaluated by the different algorithms is shown in Table 5. The bold number in each column shows the optimal minimum value in that column. Comparing the results of Table 5 with those of Tables 3 and 4, it could be conducted that the performance of the system after using the RESs has improved impressively. Table 6 shows the set of non-

Table 9
Comparison of objective functions evaluated by different methods considering RESs for 25 trails on Test system 2.

Objective function	Method	Average	Standard deviation	Worst solution	Best solution	Open switches of best solution	CPU time [s]
Power losses [kW]	GA	409.002	3.466	418.406	406.512	s8,s35,s41,s62,s85,s87,s88,s89,s90,s91,s92,s93,s94	14.445
	PSO	403.278	1.672	408.699	402.851	s8,s34,s43,s62,s85,s87,s88,s89,s90,s91,s92,s93,s94	12.145
	HBMO	408.873	3.127	416.954	406.132	s8,s34,s63,s85,s87,s88,s89,s90,s91,s92,s93,s94,s96	13.495
	The proposed algorithm	394.845	00.00	394.845	394.845	s8,s34,s41,s64,s85,s87,s88,s89,s90,s91,s92,s93,s94	11.046
Voltage deviation [p.u]	GA	0.049192	0.00111	0.051671	0.048502	s8,s35,s43,s62,s85,s87,s88,s89,s90,s91,s92,s93,s94	13.784
	PSO	0.047794	0.00031	0.048958	0.047759	s8,s12,s17,s29,s34,s43,s63,s85,s85,s88,s89,s90,s94	11.298
	HBMO	0.049001	0.00077	0.050878	0.048181	s8,s35,s40,s64,s84,s85,s87,s88,s89,s90,s91,s93,s94,s96	11.823
	The proposed algorithm	0.045230	0.00000	0.045230	0.045230	s8,s42,s44,s62,s73,s77,s84,s85,s90,s91,s93,s94,s95	10.824
Cost [$]	GA	1,157.934	1.086	1,160.041	1,157.260	s8,s34,s37,s64,s41,s56,s65,s87,s88,s89,s90,s91,s92	15.903
	PSO	1,155.601	0.342	1,156.29	1,155.339	s8,s35,s85,s87,s88,s89,s90,91,s92,s93,s94,s96,s97	13.857
	HBMO	1,156.900	0.523	1,158.106	1,156.455	s8,s35,s38,s56,s84,s87,s88,s89,s90,s91,s93,s96,s97	14.45
	The proposed algorithm	1,153.954	00.00	1,153.954	1,153.954	s8,s34,s85,s87,s88,s89,s90,s91,s92,s93,s94,s96,s97	11.293
Emission [lb]	GA	333,931.7	433.4	335,094.9	333,731.4	s8,s35,s38,s42,s56,s64,s87,s88,s89,s90,s91,s92,s93	14.364
	PSO	332,835.5	280.4	333,718.7	332,631.7	s8,s39,s47,s85,s87,s88,s89,s90,s91,s92,s93,s96,s97	11.742
	HBMO	333,387.4	338.1	334,371.4	333,187.7	s34,s38,s83,s85,s86,s87,s88,s89,s90,s91,s93,s96,s97	13.586
	The proposed algorithm	331,303.6	000.0	331,303.6	331,303.6	s5,s14,s35,s39,s44,s86,s88,s90,s91,s92,s93,s96,s97	10.934

Table 10
Some of the non-dominated-solution found for MDFR problem (Test system 2).

	Power losses (kW)	Voltage deviation (pu)	Cost ($)	Emission (lb)
1	394.845	0.0518573	1,155.617	354,055.00
2	411.635	0.0511236	1,159.601	339,811.14
3	418.340	0.0507539	1,159.301	342,031.88
4	434.698	0.0518089	1,156.824	352,753.40
5	470.137	0.0452303	1,157.585	354,907.74
6	421.103	0.0575129	1,160.041	338,810.85
7	443.167	0.0574801	1,161.901	336,764.20
8	423.218	0.0493687	1,159.298	343,783.64
9	432.495	0.0575949	1,161.843	336,927.69
10	434.013	0.0518284	1,157.458	350,705.02
11	484.735	0.0613938	1,153.954	370,825.78
12	423.502	0.0499521	1,158.755	345,848.50
13	463.612	0.0597616	1,155.460	361,918.89
14	428.347	0.0486935	1,157.582	349,087.17
15	425.001	0.0581013	1,159.491	341,750.19
16	535.687	0.0597561	1,167.844	331,303.69
17	421.624	0.0505263	1,158.129	345,749.57
18	442.959	0.0487904	1,161.286	338,745.86
19	448.565	0.0501727	1,155.881	360,702.48
20	428.347	0.0486935	1,157.582	349,087.17

dominated solutions found for MDFR problem considering RESs. Each of these solutions can be the best one, depending on the pre-specified priorities by decision maker. For example, if the main goal is to minimize the power losses, so, the operator should select the best solution from the first column of Table 6. It should be noted in this table, the behavior of each objective function is related to the behaviors of the other objective functions. In order to see this relationship more clearly, along with Figs. 4–7, in Table 7, the results of different combinations of the objective functions are considered as follows:

Case I: Considering function f_1 (neglecting f_2, f_3 and f_4)
Case II: Considering function f_2 (neglecting f_1, f_3 and f_4)
Case III: Considering function f_3 (neglecting f_1, f_2 and f_4)
Case IV: Considering function f_4 (neglecting f_1, f_2 and f_3)
Case V: Considering functions f_1, f_2 and f_3 (neglecting f_4)
Case VI: Considering functions f_1, f_3 and f_4 (neglecting f_2)
Case VII: Considering functions f_2, f_3 and f_4 (neglecting f_1)
Case VIII: Considering functions f_1, f_2 and f_4 (neglecting f_3)
Case IX: Considering functions f_1, f_2, f_3 and f_4

As mentioned in Section 5, a fuzzy clustering technique is used to control the size of the repository. Also, in this paper a fuzzy decision making procedure is adopted to obtain "most-preferred" solution. In order to aim this goal, the importance of each objective function, i.e. w_i, should be specified, such that $\sum_{i=1}^{4} w_i = 1$.

To have better comparison between the single objective and multiobjective optimization, the results of the single objective optimization cases (cases I–IV) as well as the multiobjective optimization cases (cases V–IX) are shown in Table 7. In the cases V–IX, the total emission, the voltage deviation, the total power losses and the total cost objective functions are neglected, respectively. In the first part of Table 7 (cases I–IV), the value of each objective function after applying single optimization is shown. The results show that in some cases the improvement of an objective function will affect the other objective functions in the same manner while it may negatively influence another objective function. Some of the most important results which can be inferred from this table are as follows:

- From Table 7, we can find that in a large range of variation, the behavior of f_2 (voltage deviation) and f_4 (emission) are the same; that is when f_2 is minimized individually, f_4 is also minimized and when it increases the other one will increase, too.

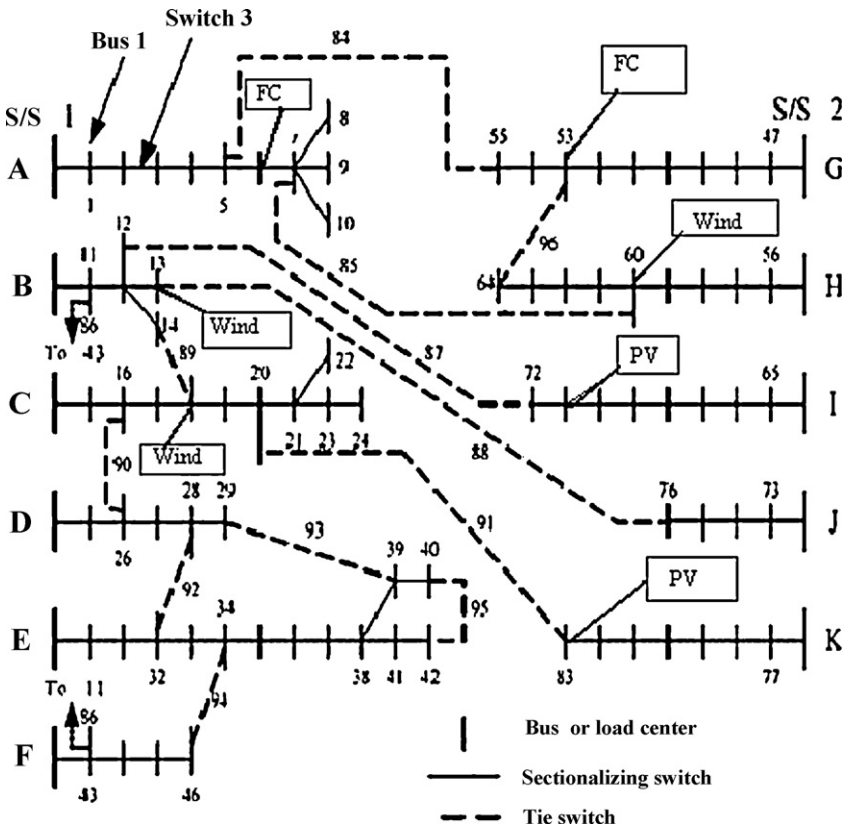

Fig. 8. Single line diagram of 85 bus test system.

The evidence of this claim is the results of the cases VII, VIII, IX. In case VII, in the 2nd and 4th row, when the weighting factor of f_2 and f_4 is increased (so increasing their importance in the optimization when neglecting f_1) the value of these two objective functions is the same ($f_2 = 0.050984$ p.u; $f_4 = 27{,}776.86$ lb). This happens similarly in case VIII, in the 2nd and 3rd row ($f_2 = 0.048988$ p.u; $f_4 = 25{,}335.31$ lb), and in case IX, in the 2nd and 4th row ($f_2 = 0.0489880$ p.u; $f_4 = 25{,}335.31$ lb).

- From this table, it can be deduced that f_3 (total cost) has a conflicting behavior to the other three objective functions especially f_2 and f_4. In case VI (neglecting voltage deviation objective function), increasing the importance of f_3 (by increasing w_3), has a

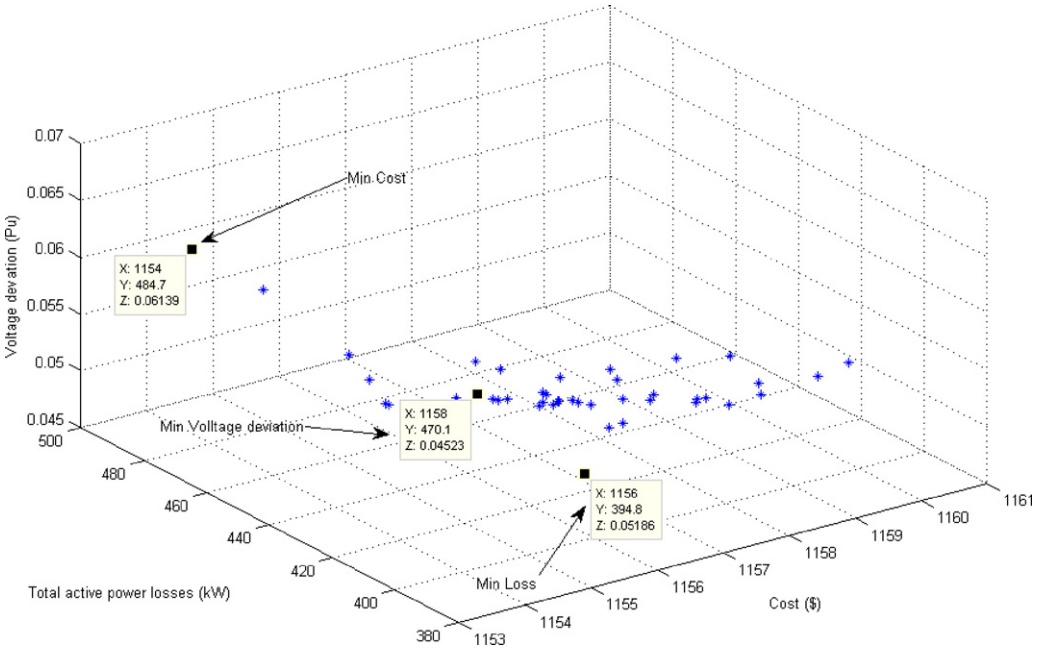

Fig. 9. 3D plot of the Pareto-optimal solutions found for case study 2 considering total active power losses, voltage deviation and cost objective functions.

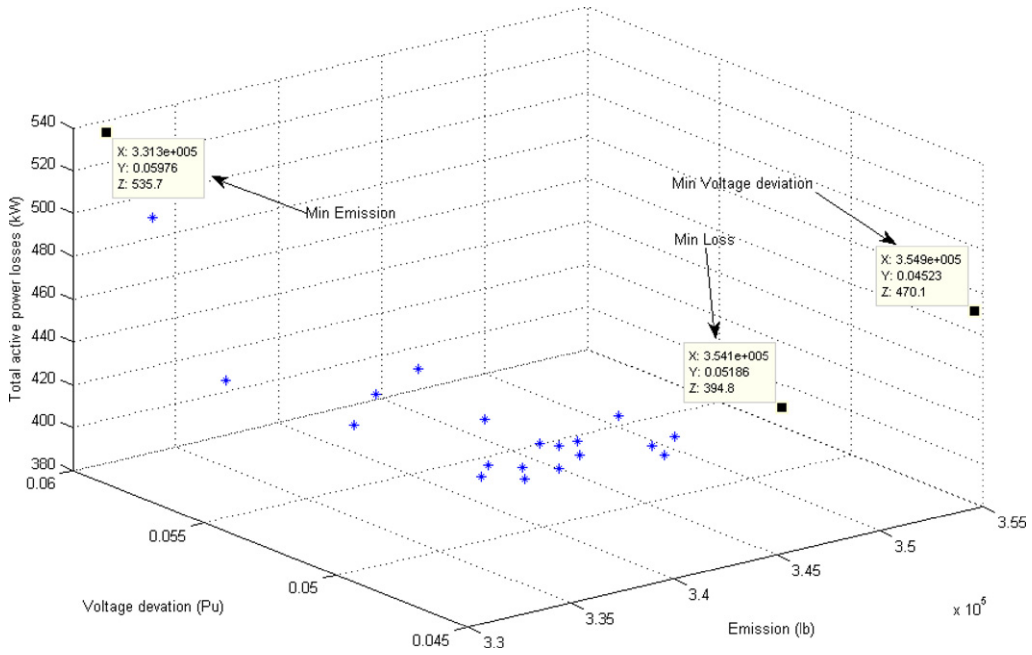

Fig. 10. 3D plot of the Pareto-optimal solutions found for case study 2 considering total active power losses, voltage deviation and emission objective functions.

negative effect on the other two objective functions (f_1 and f_4). Similarly in case VII, the increasing importance of f_2 and f_4 (w_2 and w_4) has resulted in the same solution, while the same increase in the importance of f_3 has resulted in a different solution which shows a conflicting behavior with respect to the other two objective functions. The same observation can be inferred from case IX.

- The dependency of f_1 (total power losses) versus the other functions is to some extent weak. From case V it can be figured out that f_1 has a similar behavior with f_2 while the confliction with f_3 (as mentioned before) is evident. In case VI, it shows the same behavior with f_4. But in case VIII, a different conflicting behavior on both f_2 and f_4 can be seen. Similarly in case IX, f_1 is in contrast with the other objective functions. Therefore, it can be deduced that f_1 behavior in progress is not in direct relationship with f_2 and f_4.
- In case IX, 3rd row, the main importance among the four objective functions is applied to the cost function (f_3). Nevertheless, the value of this objective function (cost) is more than that of case III. In fact this difference in the cost values of the two cases indicates the extra value which must be paid as the cost of decreasing the total active power losses as well as enhancing the security level (voltage deviation) and reducing the total emission.
- As before-mentioned, each Pareto solution of the repository is indicative of an alternative option for the system operator as a decision maker. Indeed, after applying all the limitations and

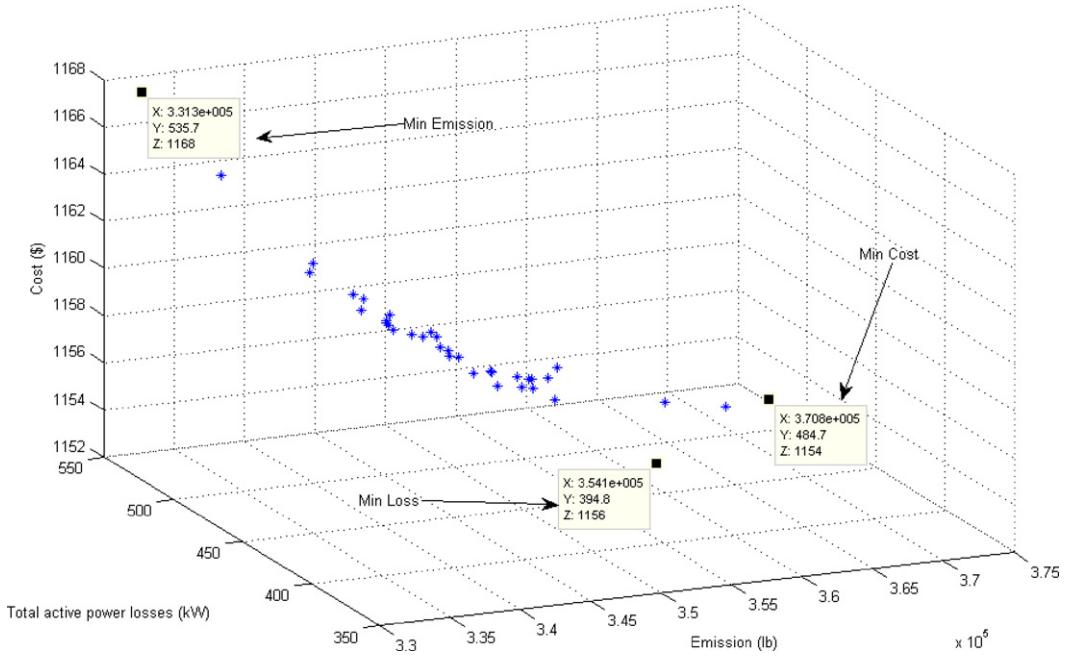

Fig. 11. 3D plot of the Pareto-optimal solutions found for case study 2 considering total active power losses, emission and cost objective functions.

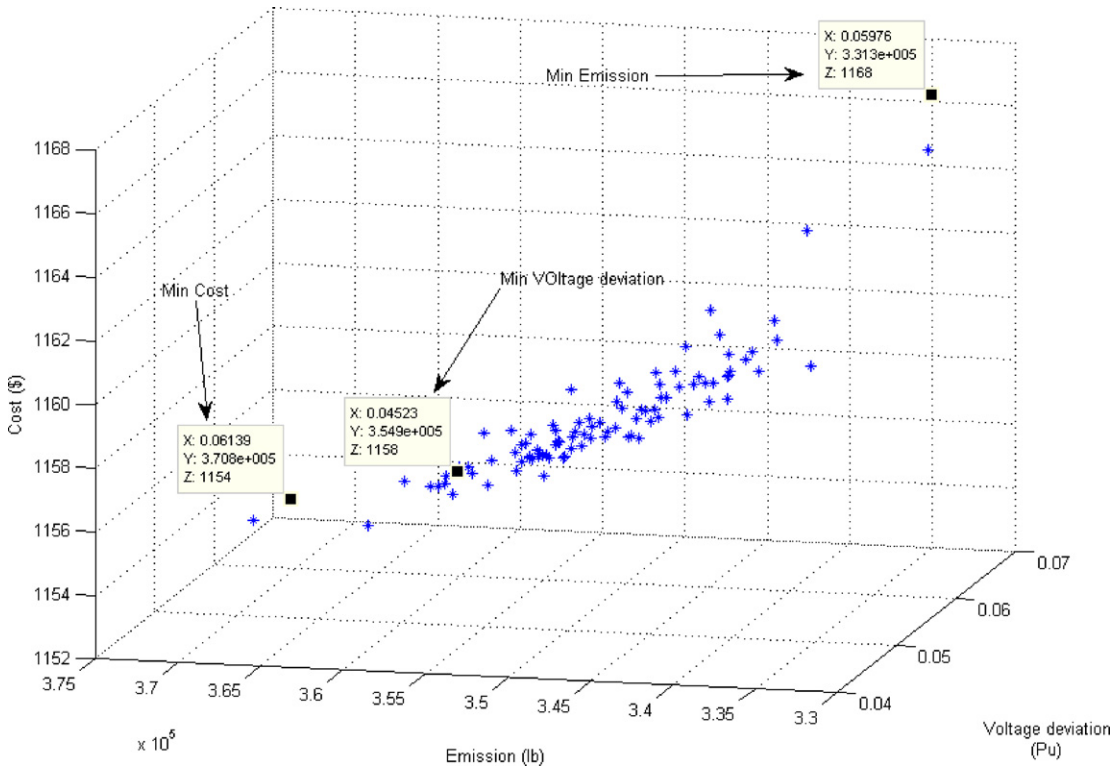

Fig. 12. 3D plot of the Pareto-optimal solutions found for case study 2 considering emission, voltage deviation and cost objective functions.

conditions which is determined by the operator as the requirements of the system, it is needed to extract the best compromised solution according to the preferences among the stored solutions of the repository. It can be seen in case IX of Table 7 that with the same preferences of the objective functions, the best compromised solution is 94.805 kW, 0.0489880 p.u, 158.429$ and 25,335.31 lb for f_1, f_2, f_3 and f_4, respectively.

Neglecting f_4, f_2, f_1 and f_3 in the multiobjective optimization, the best compromised solution can be achieved from the first row of the cases V to VIII, respectively.

To show the improvement of each objective function with respect to the other objective functions, the three-dimensional (3D) plot of the non-dominated solutions of the multiobjective DFR problem are shown in Figs. 4–7. Each star denotes a Pareto-optimal solution in these figures. The dependency of each objective function improvement to the other objective functions can be seen in these figures, too.

7.2. Case study 2

The second case study is a standard 11.4 kV radial distribution system which is consisted of 2 substations, 11 feeders and 85 buses and 96 switches [34]. The initial active power loss and maximum voltage deviation neglecting RESs are 531.99 kW and 0.052 p.u, respectively. In Table 8, the location, capacity and the type of each RES are shown. The single diagram of the second test system is depicted in Fig. 8.

To understand the behavior of each objective function with respect to the others, in Table 7 the results of a complete investigation is shown and explained. So, in order to avoid unnecessary comparisons in case study 2, the performance of the proposed algorithm is assessed in the presence of RESs.

In Table 9, the complete comparison between the values of all objective functions is implemented. All the objective functions have improved effectively and the satisfying performance of the proposed method is evident. Also, by comparing the values of the standard deviation, mean value, time of the run and the worst solution found by each algorithm, the superiority of the proposed algorithm is verified.

Some of the non-dominated solutions found in multiobjective DFR problem considering the RESs are shown in Table 10. In order to see the behavior of each objective function according to the others, in Figs. 9–12 the three-dimensional (3D) plot of the non-dominated solutions are shown. Each star denotes a Pareto-optimal solution. The stars which are shown by rectangular box in the figure are optimal solutions which are found during single optimization of each of the objective functions.

8. Conclusion

In this paper an appropriate modified algorithm based on HBMO (MHBMO) algorithm is introduced to solve the multiobjective DFR problem considering RESs. The objective functions consist of the total active power losses, the voltage deviation of each bus from its nominal value, the total cost of the system (including the grid and the RESs) and the total emission produced by the system. In the proposed method, a set of non-dominated solutions called Pareto-optimal solutions are found and stored in the repository which its size is controlled by the use of fuzzy clustering method. Also a fuzzy-based decision maker was introduced to select the 'best' compromised solution according to his/her experiences and preferences. To improve the original HBMO algorithm, the mating process is enhanced so that to improve the exploration ability of the algorithm in the entire search space. In order to see the feasibility and ability of the proposed method, MHBMO algorithm is applied to two test systems and the results are compared by some of the most famous optimization algorithms. The results show the good performance and credibility of the proposed method in the MDFR problem. Also it was shown that the behaviors of the voltage

deviation and total emission objective functions are similar to each other while the cost objective function has a conflicting behavior regarding the other objective functions. Also, the superiority of the proposed method is shown with respect to the other optimization methods in the area.

References

[1] M. Tanrioven, J. Power Sources 150 (2005) 136–149.
[2] A.U. Dufour, J. Power Sources 71 (1998) 19–22.
[3] Ph. Thounthong, V. Chunkag, P. Sethakul, S. Sikkabut, S. Pierfederici, B. Davat, J. Power Sources 196 (2011) 313–324.
[4] F. Jurado, M. Valverde, A. Cano, J. Power Sources 129 (2004) 170–179.
[5] P.B. Tarman, J. Power Sources 61 (1996) 87–89.
[6] R.J. Braun, S.A. Klein, D.T. Reindl, J. Power Sources 158 (2006) 1290–1305.
[7] T. Niknam, A.M. Ranjbar, A.R. Shirani, IFAC Conf. Korea, vol. 3, 2003, pp. 1105–1110.
[8] M.Z. Jacobson, Energy Environ. Sci. (2009) 1–55.
[9] C.M. Lin, M. Gen, Expert Syst. Appl. 34 (4) (2008) 2480–2490.
[10] P.C. Chang, S.H. Chen, Liu. Sub, Expert Syst. Appl. 33 (3) (2007) 762–771.
[11] D. Debaprya, IEEE Trans. Power. Deliv. 21 (1) (2006) 202–209.
[12] T. Taylor, D. Lubkeman, IEEE Trans. Power. Deliv. 5 (3) (1990) 239–245.
[13] H. Kim, Y. Ko, K.H. Jung, IEEE Trans. Power. Deliv. 8 (3) (1993) 1356–1366.
[14] M.A. Kashem, V. Ganapathy, G.B. Jasmon, Transm. Distrib. 146 (1999) 563–567.
[15] M.E. Baran, F.F. Wu, IEEE Trans. Power. Deliv. 4 (2) (1989) 1401–1407.
[16] Q. Zhou, D. Shirmohammadi, W.H.E. Liu, IEEE Trans. Power. Syst. 12 (2) (1997) 724–729.
[17] T. Niknam, Energy Convers. Manage. 50 (8) (2009) 2074–2082.
[18] T. Niknam, Eur. Trans. Electr. Power 20 (5) (2010) 575–590.
[19] T. Niknam, Cybern. Syst.: Int. J. 40 (6) (2009) 508–527.
[20] T. Niknam, H.Z. Meyman, H.D. Mojarrad, A novel multiobjective fuzzy adaptive chaotic PSO algorithm for optimal operation management of distribution network with regard to fuel cell power plants, Eur. Trans. Electr. Power, in press, DOI: 10.1002/etep.525.
[21] T. Niknam, Energy Convers. Manage. 49 (2008) 3417–3424.
[22] T. Niknam, Cybern. Syst.: Int. J. 40 (6) (2009) 1–20.
[23] C. Bernay, M. Marchand, M. Cassir, J. Power Sources 108 (2002) 139–152.
[24] R.M. Moore, K.H. Hauer, G. Randolf, M. Virji, J. Power Sources 162 (2006) 302–308.
[25] L. Palma, M.H. Todorovic, P.N. Enjeti, IEEE Trans. Ind. Electr. (2009) 20–27.
[26] P.P. Singh, S. Singh, Renew. Energy 35 (2010) 563–569.
[27] T. Niknam, J. Power Zhejiang Univ. Sci. A 9 (12) (2008) 1753–1764.
[28] T. Niknam, J. Zhejiang Univ. Sci. A 9 (2008) 1753–1764.
[29] S.K. Goswami, S.K. Basu, IEEE Trans. Power. Deliv. 7 (3) (1992) 1484–1491.
[30] F. Vanderson Gomes, S. Carneiro, J.L.R.M.P.V. Pereira, P.A.N. Garcia, L. Ramos Araujo, IEEE Trans. Power. Syst. 20 (3) (2005) 1373–1378.
[31] T. Niknam, E. Azad Farsani, Sci. China Technol. Sci. 53 (2010) 950–959.
[32] T. Niknam, E. Azad Farsani, M. Nayreipour, An efficient multiobjective modified shuffled frog leaping algorithm for distribution feeder reconfiguration problem, Eur. Trans. Electr. Power, doi:10.1002/etep.473.
[33] D. Shirmohammadi, H.W. Hong, Power Syst. 4 (1) (1998) 1492–1498.
[34] A. Ashisa, D.S. Das, A. Pahwa, IEEE Trans. Power. Syst. 22 (3) (2007) 1101–1111.